

Optimal hydroponic growth of *Brassica oleracea* at low nitrogen concentrations using a novel pH-based control strategy

Ignatius Leopoldus van Rooyen

Optimal hydroponic growth of *Brassica oleracea* at low nitrogen concentrations using a novel pH-based control strategy

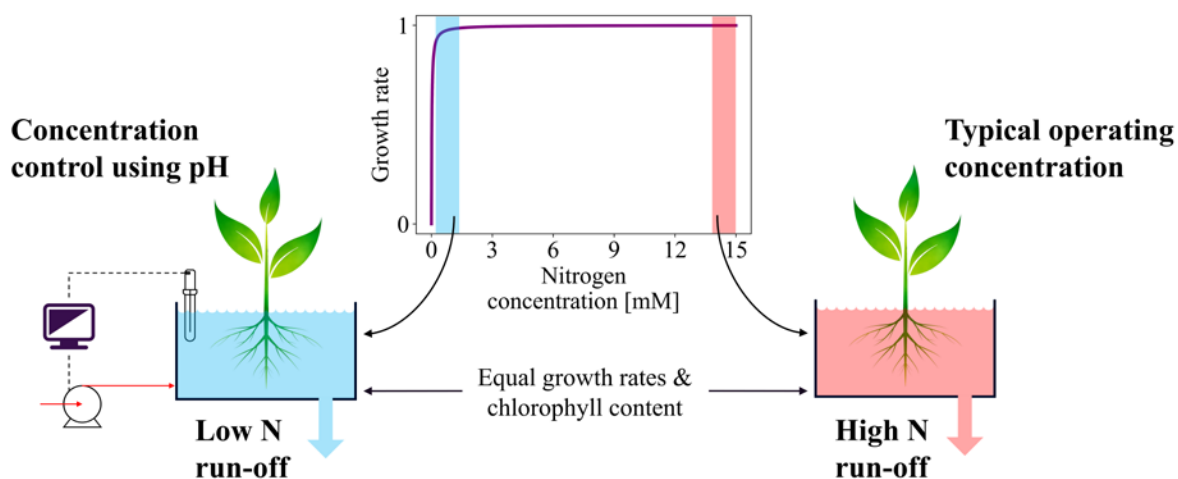
A dissertation submitted as a requirement for the degree Master of Engineering.

Ignatius Leopoldus van Rooyen
Department of Chemical Engineering
University of Pretoria

Under the supervision of Professor Willie Nicol

15 February 2021

Optimal hydroponic growth of *Brassica oleracea* at low nitrogen concentrations using a novel pH-based control strategy



Synopsis

Aquatic nitrogen pollution from conventional agriculture contributes severely to the degradation of numerous ecosystems and is considered one of the main contributors to earth's alarming rate of biodiversity loss. Soilless agriculture, in contrast to conventional agriculture, has the advantage of discharge control since the nutrient solution is contained. However, periodic replacement of the nutrient solution is dictated by inert build-up over time resulting from transpiration. As the spent solution is usually dumped, the nutrient concentrations are proportional to the load of nutrient spillage to the environment. This study investigates a novel pH-based control strategy to minimise the nitrate concentration while maintaining optimal plant growth and nutrition. Experiments were performed where the nitrate concentration was controlled at 11 mM (representing standard protocol), 1 mM, 0.5 mM, and 0.1 mM. This was accomplished by controlling the pH with a mixture of HNO_3 and NaNO_3 . A molar ratio of 3:2 ($\text{HNO}_3:\text{NaNO}_3$) resulted in relatively stable nitrate profiles with slow depletion of nitrate in solution, owing to a near-constant ratio between proton dosing required for pH homeostasis and

nitrate absorption. Small manual corrections were made for the 1 mM and 0.5 mM runs, accounting for 8% of the total nitrate absorbed. For the 0.1 mM run, instead of manual correction, an automatic nitrate addition strategy was incorporated, in which nitrate extinction was inferred from a reduction in the rate of change of pH. Zero reduction in plant growth rate and leaf chlorophyll content was detected when comparing the 11 mM run with the other runs, indicating optimal hydroponic performance. A novel nitrate control algorithm is presented that uses pH measurement as the sole input. The experimental results and the control algorithm provide encouraging alternatives for reducing nitrogen spillage from soilless agriculture.

Keywords: Proton to nitrate ratio; Nitrate concentration control; Nitrogen spillage; Soilless agriculture

Contents

Synopsis	ii
List of Figures	v
Nomenclature	viii
1. Introduction	1
2. Theory	3
2.1 The nitrogen cycle	3
2.2 Hydroponics	4
2.2.1 The hydroponic nutrient solution	5
2.2.3 Nitrogen pollution from hydroponic systems	7
2.3 pH characteristics of plants	9
3. Experimental	11
3.1 Overview of experimental setup	11
3.2 Method and planning	13
3.3 Apparatus and instruments	15
4. Results and discussion	17
4.1 Relating nitrate absorption to proton dosing	17
4.2 Controlling pH and nitrate concentration simultaneously using a single dosing reservoir	18
4.3 Automatic prevention of nitrate depletion using a second dosing reservoir	22
5. Conclusions	27
References	28
Appendix	35

List of Figures

- Figure 1:** Illustration of the natural nitrogen cycle with synthetic nitrogen input. 4
- Figure 2:** Illustration of plant root exudates associated with pH changes. Exudates not associated with nutrient uptake are grouped as “ $\text{COOH}^- \text{H}^+$ ”. 10
- Figure 3:** Annotated photo of the experimental setup. Shown are four independent hydroponic systems each hosting a single Kale plant, labelled “plant 1” to “plant 4” from right to left. 11
- Figure 4:** Simplified process flow and instrumentation diagram of the setup showing major control elements, vessels, and dosing bottles. 12
- Figure 5:** Sequential function chart of the control algorithm responsible for the flood-and-drain mechanism (switching P4 on and off), liquid level control (first horizontal branch), pH control (second branch) and nitrate extinction prevention (bottom branch). “*sp.*” corresponds to a set point of 1.8 L. 15
- Figure 6:** Results from run 1 using Hoagland’s solution with frequent replacement (average nitrate concentration of 12 mM). The pH was controlled at an average value of 6.05 ($\sigma = 0.07$, $n = 997$). HCl dosing rates (a), nitrate absorption rates (b) and transpiration rates (d) all exhibit an exponential increase. Subplot (c) relates proton dosing to nitrate absorption where a fitted value of $\eta = 0.49$ is obtained. 19

- Figure 7:** Results from runs 2 to 4. Nitrate controlled at approximately 1 and 0.5 mM for runs 3 and 4, respectively. All runs used the same dosing solution composed of 0.3 M HNO₃ and 0.2 M NaNO₃ ($\alpha = 0.6$ mol mol⁻¹). For runs 3 and 4, manual corrections were made with NaNO₃ as indicated by bar plots in (b) and (c). Vertical dotted lines indicate solution replacement. 21
- Figure 8:** Subplots (a), (b) and (c) provide logarithmic plots of the dosing rates (D_R) for runs 2 to 4. The slopes of the fitted lines equal the RDR values. Subplot (d) gives RDR and RGR as a function of the nitrate operating concentration. Error bars span the data range (min. ↔ max.) of the four plants. 22
- Figure 9:** Results from run 5. Shown are profiles of ∇pH divided by the running average of ∇pH . As described in Figure 8, NaNO₃ dosing (from B2 in Figure 4) occurs when there is a 70% reduction in ∇pH , whereupon 0.2 mmol NaNO₃ L⁻¹ solution is dosed. Also shown, are the measured nitrate concentrations in solution. 25
- Figure 10:** Comparison of leaf chlorophyll content and root mass fraction of runs 2 to 5. Also shown are average values of the growth parameters RGR and RDR for runs 2 to 4, which are compared against the growth parameters for run 5 (20% more light was received) in two separate annotations. Error bars span the data range (min. ↔ max.) of the four plants. 26
- Figure A1:** Detailed drawing of the nutrient solution reservoir. Side view on left, top view on right. 36

Figure A2:	Detailed drawing of the plant vessel. Side view on left, top view on right.	36
Figure A3:	Detailed drawing of the sand filter. Side view on left, top view on right.	37
Figure A4:	Circuit diagram of control system.	39

Nomenclature

D_R	dosing rate of the acid-nitrate solution used for pH control (B1 in Figure 4).	mmol-NO ₃ day ⁻¹
FW	plant fresh mass.	g
n	number of sample points.	#
RDR	relative dosing rate = $\frac{\ln(D_{R,t}) - \ln(D_{R,t+\Delta t})}{\Delta t}$	day ⁻¹
RGR	relative growth rate = $\frac{\ln(FW_t) - \ln(FW_{t+\Delta t})}{\Delta t}$	day ⁻¹
$sp.$	set-point.	
t	time.	day
α	proton-to-nitrate ratio in the acid-nitrate solution used for pH control (B1 in Figure 4).	mol mol ⁻¹
η	ratio of “proton dosing required for pH homoeostasis” to “nitrate absorbed by the plant”.	mol mol ⁻¹
∇pH	absolute rate of change of pH with respect to time $\left(\frac{\Delta pH}{\Delta t}\right)$.	pH day ⁻¹
σ	standard deviation.	

1. Introduction

Nitrogen is an essential element for plant growth. To meet the world-population's food demands, conventional agriculture relies on high nitrogen application rates (Bijay-Singh et al., 1995; Chao and Pei Fang, 2008). Although attaining high plant growth, this practice exhibits low nitrogen use efficiency and is environmentally hazardous with around 50% loss of nitrogen through system boundaries. The resulting environmental impacts range from eutrophication and air pollution to biodiversity loss, climate change and stratospheric ozone depletion (Andersen and Kristiansen, 1983; Bijay-Singh et al., 1995; Chen et al., 2008; Gustafson, 1983; Isermann, 1990; Kanter et al., 2020).

Soilless agriculture, where nutrients are contained within a well-administered aqueous solution, can alleviate many of the problems of conventional agriculture (Christie, 2004; Ruffi-Salis et al., 2020). However, the nutrient solution accumulates salinity and toxic substances quickly due to transpiration and is usually discharged periodically despite having high nutrient concentrations. As a result, the release of nitrogen to the environment is intensified (Bugbee, 2004; del Amor and Porras, 2009; Kumar and Cho, 2014; Prystay and Lo, 2001; Silberbush and Ben-Asher, 2001).

Typical nutrient solutions contain from 12 mM to 15 mM nitrogen (Arnon and Hoagland, 1940; Cooper, 1988; Hewitt, 1996; Steiner, 1984), which is roughly two orders of magnitude higher than the limiting concentration at which symptoms of nitrogen deficiency manifest (Hellgren and Ingestad, 1996; Li et al., 2015; Kuzyakov and Xu, 2013; Le Deunff, 2019; Wang, 2012). As plants consume nitrogen quickly, these high concentrations safeguard against nitrogen depletion and hence deficiency. However, when the nutrient solution is discarded, much more nitrogen is spilled than necessary. Many efforts have been successful

at controlling nitrogen concentration at lower levels, primarily using ion-selective-electrodes (Cho et al., 2018; Kim et al., 2013). However, this strategy is expensive and poses problems such as signal drift and reduced accuracy over time (Bugbee, 2004; Christie, 2004). Other efforts have made use of the electrical conductivity of the nutrient solution to control the total nutrient concentration (Christie, 2004; Domingues et al., 2012). Although cheap and easily implemented, as individual nutrient concentrations are not measured, this approach can lead to nutrient imbalances. Furthermore, the measurement signal is mostly induced by calcium, magnesium and sulphate remaining in solution (Bugbee, 2004; Lenord Melvix and Sridevi, 2014). So rather than risk nitrogen deficiency, excessive nitrogen is still employed (Goins et al., 2004).

This study endeavoured to use pH as the sole input to control the nitrate concentration in solution at lower levels. As pH control is standard protocol in most hydroponic systems, the aim was to develop a nitrate-control methodology that does not require any additional measurement apparatus.

When nitrate is supplied as the sole nitrogen source, the pH rises, and acid dosing is required for pH homeostasis. This can be attributed to the release of OH^- ions and the absorption of H^+ ions upon nitrate assimilation (Dijkshoorn, 1962). The theoretical ratio of 1 OH^- ion released per nitrate ion assimilated is typically not reflected in the solution pH since numerous other uptake and exudation effects (such as carboxylic acid exudation) cause pH changes (Dijkshoorn, 1962; Imsande, 1986; Smith and Raven, 1979). The premise of this study is to use the overall pH response and acid dosing characteristics during crop growth to infer the nitrate assimilation rate. Nitrate concentration control can then be achieved by feeding nitrate at the same rate. This study thoroughly investigates the above notion and suggests additional control schemes to compensate automatically for errors in the predicted rates.

2. Theory

2.1 The nitrogen cycle

Nitrogen recycling between the atmosphere, biosphere and hydrosphere is intimately connected to all living creatures on earth. Proteins and nucleic acids contain a significant fraction of nitrogen and hence nitrogen is key to life on our planet. There is an abundance of nitrogen in the atmosphere, but it is in the form of the relatively inert gas, N_2 , and must be converted into NO_3^- or NH_4^+ before plants can utilize it (Burris, 2001). Prior to the invention of the Haber-Bosch process, all nitrogen transfer from the atmosphere to the biosphere (microbial nitrogen fixation) was facilitated by prokaryotes, which tightly regulated the influx of bio-available nitrogen (ammonia and nitrate) into the soil, as shown in Figure 1 (Miles et al., 1992). Nitrogen fixation is energy intensive, however, and fixed nitrogen is often the limiting nutrient for plant growth (Burris, 2001; Miles et al., 1992). Due to the world population's high demands for food, most of the nitrogen fixed today is accomplished by the Haber-Bosch process, which reduces N_2 to ammonia catalytically at high temperatures and pressures using fossil fuel combustion (Burris, 2001). The input of synthetic nitrogen powered the "green revolution" and contributed directly to the explosion of the human population in the previous century (Erisman et al., 2008). The availability of relatively cheap synthetic nitrogen has led to significant spillage of nitrogen to the environment and thus interference with the natural nitrogen cycle. Synthetic nitrogen enters the hydrosphere primarily via agricultural run-off, with approximately 50% of the applied nitrogen being lost through system boundaries (Chen et al., 2008; Delgado, 2002; Eickhout et al., 2006; Kanter et al., 2020). The resulting environmental impacts include eutrophication, biodiversity loss, climate change and stratospheric ozone depletion (Kanter et al., 2020). As water flow through crop fields is difficult to control, and synthetic nitrogen remains relatively cheap,

the application of excess nitrogen remains the economically favourable option (Goins et al., 2004).

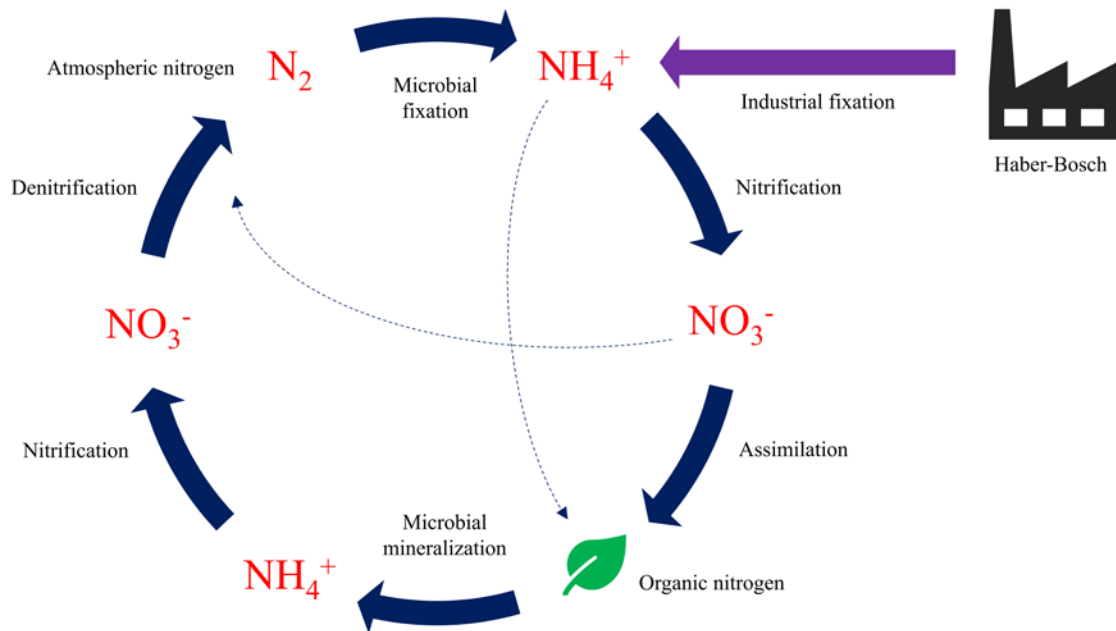


Figure 1. Illustration of the natural nitrogen cycle with synthetic nitrogen input.

2.2 Hydroponics

The primary difference between hydroponics and conventional agriculture is that hydroponics does not involve the use of soil. Plant roots are instead immersed in an aqueous solution that contains all the nutrients required for growth. The hydroponic industry is growing rapidly worldwide, especially for producing vegetable greens in a changing world where human nutrition has become topical (Mathias, 2014; Miller et al., 2020). Hydroponics claim several advantages over conventional agriculture, such as lower water consumption, freedom from soil-borne diseases and pests, and high plant growth rates (Kumar and Cho, 2014; Rufi-Salis et al., 2020; Seungjun and Jiyoung, 2015). From an environmental perspective, the nutrient solution is physically contained and thus run-off can be controlled.

2.2.1 The hydroponic nutrient solution

Tables 1 and 2 list the essential elements found in hydroponic nutrient solutions. Table 2 specifically lists the micro-nutrients, which are required in much smaller quantities by plants as compared with the macro-nutrients, which are listed in Table 1.

Table 1: Absorbable ionic forms of macro-nutrients (Trejo-Téllez & Gómez-Merino, 2012)

Macro-nutrient	Absorbable forms
N	NO_3^- , NH_4^+
P	H_2PO_4^- , HPO_4^{2-} , PO_4^{3-}
K	K^+
Ca	Ca^{2+}
Mg	Mg^{2+}
S	SO_4^{2-}

Table 2: Absorbable ionic forms of micro-nutrients (Trejo-Téllez & Gómez-Merino, 2012)

Micro-nutrient	Absorbable forms
B	$\text{H}_2\text{BO}_3^{2-}$
Na	Na^+
Cl	Cl^-
Cu	Cu^{2+}
Fe	Fe^{2+} , Fe^{3+}
Mn	Mn^{2+}
Mo	MoO_4^{2-}
Zn	Zn^{2+}

Table 3 lists the nutrient concentrations found in typical hydroponic solutions as tabulated by Trejo-Téllez & Gómez-Merino (2012).

Table 3: Elemental composition of nutrient solutions as suggested by selected authors. All values are given in ppm (mg element L⁻¹)

Nutrient	Hoagland & Arnon (1938)	Hewitt (1966)	Cooper (1979)	Steiner (1984)
N	210	168	200-236	168
P	31	41	60	31
K	234	156	300	273
Ca	160	160	170-185	180
Mg	34	36	50	48
S	64	48	68	336
Fe	2.5	2.8	12	2-4
Cu	0.02	0.064	0.1	0.02
Zn	0.05	0.065	0.1	0.11
Mn	0.5	0.54	2	0.62
B	0.5	0.54	0.3	0.44
Mo	0.01	0.04	0.2	N/A

The nutrient concentrations in Table 3 were formulated based on the ionic strength of the solution and the relative uptake rates of the individual nutrients. For example, nitrogen is supplied in the highest concentration as it is taken up at the highest rate. The ionic strength is an index of the total concentration of dissolved ions and the osmotic pressure of the solution, which significantly affects plant growth, development, production, and water uptake (Hosseinzadeh et al, 2017; Steiner, 1984; Trejo-Téllez & Gómez-Merino, 2012). Hence, the formulations are optimized for maximum nutrient availability (high concentrations), yet do not exceed concentrations at which adverse effects would manifest. The ionic strength of the solution is often referred to as the electrical

conductivity (EC) as these two properties are proportional and the EC is easily measured. Typical ECs employed in hydroponic solutions range between 1.5 dS m⁻¹ and 2.5 dS m⁻¹ (Hosseinzadeh et al, 2017).

Besides nutrients, the nutrient solution must be mildly acidic (pH ≈ 6), contain dissolved oxygen, and be continuously mixed for optimal cultivation. Several different hydroponic systems have been developed to meet these requirements. Common systems include the Nutrient-Film-Technique and the Ebb-and-Flow (flood-and-drain) system (Trejo-Téllez & Gómez-Merino, 2012). As plants consume dissolved oxygen, these systems primarily induce a constant gas-liquid mass transfer of oxygen and allow good mixing of the nutrient solution around the root zone.

The pH of the nutrient solution changes significantly as the plants absorb nutrients. The rate of change of pH depends strongly on the choice and proportions of nutrients supplied, but aggressive pH control is required for most formulations. The optimum pH of a nutrient solution depends on the type of crop, but a pH value of 5.8 – 6.2 is commonly employed (Trejo-Téllez & Gómez-Merino, 2012). Furthermore, the availability of nutrients to the plant depends on pH. For example, plants can absorb ammonium (NH₄⁺) but not ammonia (NH₃). At a pH of around 12, only NH₃ is present in the solution and at a pH of around 6, only NH₄⁺ is present (Trejo-Téllez & Gómez-Merino, 2012). Furthermore, Fe²⁺, Mn²⁺, PO₄³⁻, Ca²⁺ and Mg²⁺ tend to precipitate above a pH of 7. Below a pH of 4, plant roots are damaged (Hosseinzadeh et al, 2017).

2.2.2 Nitrogen pollution from hydroponic systems

Plants transpire a lot of water, and water addition is required to maintain the solution volume. This ultimately results in a build-up of salinity and inert species in the nutrient solution over time. Also, plants exude toxic substances which are intended to cause detrimental effects to neighbouring plant species (a process known as allelopathy), which, in hydroponic systems, results in autotoxicity of the plants (Hosseinzadeh et al., 2017). Infinite recycling is thus not possible and periodic replacement of the nutrient solution is required to maintain habitable conditions. The spent solution is usually dumped without proper treatment despite having high nutrient concentrations. As a result, nitrogen spillage to the environment is intensified (Bugbee, 2004; del Amor and Porras, 2009; Kumar and Cho, 2014; Prystay and Lo, 2001; Silberbush and Ben-Asher, 2001).

As discussed, nutrient solutions are formulated to maximise nutrient concentrations, which allows for high nutrient availability and safeguards against nutrient depletion. However, when the nutrient solution is replaced, proportionally high amounts of nutrients are spilled. (del Amor and Porras, 2009; Prystay and Lo, 2001). The rate at which nitrogen is consumed by plants follows Michaelis-Menten kinetics, where the rate is constant at sufficiently high concentrations but declines at lower concentrations (Silberbush and Ben-Asher, 2001). The limiting concentration at which a significant decrease in nitrogen absorption, and hence plant growth, is observed is roughly two orders of magnitude smaller than the typical nitrogen concentration found in nutrient solutions. Thus, lower nitrogen concentrations can be employed without sacrificing plant growth and nutrition. However, as plants consume nitrogen quickly, a larger reservoir would be required, which would still result in an equal magnitude of nitrogen spillage. Alternatively, a control strategy may be employed to maintain the nitrogen concentration at lower levels. Many efforts have utilized

ion-selective electrodes to measure and subsequently control either nitrate or ammonium concentrations in solution (Cho et al., 2018; Kim et al., 2013). This strategy is expensive, however, and poses problems such as signal drift and reduced accuracy over time (Bugbee, 2004; Christie, 2004). Other efforts have made use of the electrical conductivity of the nutrient solution (Christie, 2004; Domingues et al., 2012). The solution's electrical conductivity is near-proportional to the total amount of dissolved ions (nutrients) in solution, thus, allowing for concentration control of all nutrients at lower levels. But as individual nutrient concentrations are not measured, this approach can lead to nutrient imbalances. Furthermore, the measurement signal is mostly induced by calcium, magnesium and sulphate remaining in solution (Bugbee, 2004; Lenord Melvix and Sridevi, 2014). So rather than risk nitrogen deficiency, high nutrient concentrations are still employed (Goins et al., 2004).

2.3 pH characteristics of plants

Figure 2 depicts some of the processes responsible for causing pH changes in the nutrient solution. Plant root exudates consist of numerous chemical species. The organic exudates not associated with nutrient uptake are grouped as “ $\text{COO}^- \text{H}^+$ ” in Figure 2. Some exudates tend to cause a drop in pH (such as carboxylic acids and H^+), while others (such as OH^-) tend to cause a rise in pH (Hosseinzadeh et al., 2017). When anions such as NO_3^- , SO_4^{2-} or H_2PO_4^- are taken up in higher quantities than cations (K^+ , Ca^{2+} , Mg^{2+}), the plant excretes OH^- or HCO_3^- anions to balance the electrical charges, which increases the solution's pH. This is the case when NO_3^- is supplied as the sole nitrogen source. Furthermore, there is an additional release of OH^- ions and absorption of H^+ ions upon nitrate assimilation. The combined basic effects are larger than the acidic effects caused by plant. Thus, the pH of the solutions rises when nitrate is supplied as the sole nitrogen source (Dijkshoorn, 1962; Imsande, 1986; Smith and Raven, 1979).

Alternatively, if ammonium is supplied as the sole nitrogen source, the pH decreases due to an overall higher cation uptake as the plant secretes H^+ ions to balance the electrical charge (Hosseinzadeh et al., 2017). Imsande (1986) used this approach to feed proportional amounts of ammonia and nitrate (1:4 molar) which resulted in zero pH change. Furthermore, the metabolism of neutral sugars to organic acids by plants results in an acidic effect (“ $COO^- H^+$ ” in Figure 2). Thus, when zero nitrogen is absorbed or assimilated, the pH decreases (Dijkshoorn, 1962; Imsande, 1986).

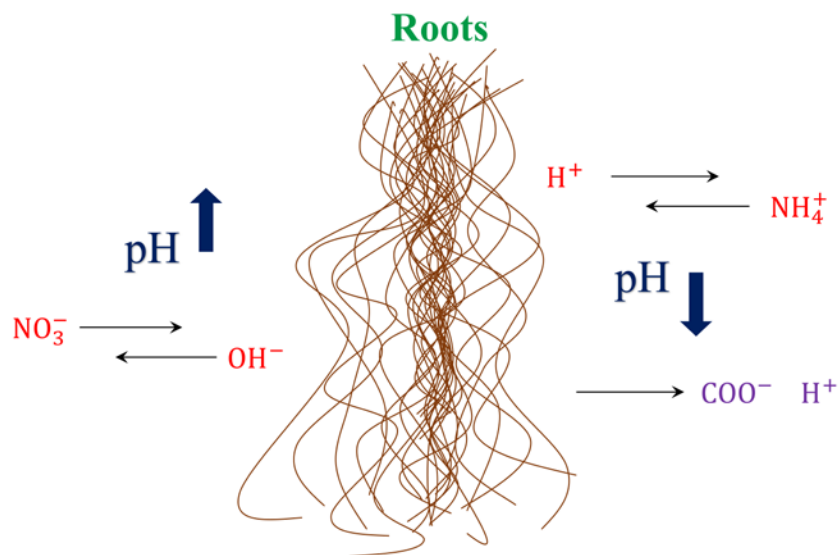


Figure 2: Illustration of plant root exudates associated with pH changes. Exudates not associated with nutrient uptake are grouped as “ $COO^- H^+$ ”.

3. Experimental

3.1. Overview of experimental setup

Figure 3 shows four independent flood-and-drain hydroponic systems, each 1.8 L and hosting a single kale plant (*Brassica oleracea* var. *sabellica*). Details on the design and construction of the setup are given in the Appendix. For each experimental run, all four systems were operated in parallel under the same conditions, analogous to four repeat runs. A total of five runs were conducted, thus 5×4 single plant runs.



Figure 3. Annotated photo of the experimental setup. Four independent hydroponic systems are shown, each hosting a single Kale plant, labelled “plant 1” to “plant 4” from right to left.

Figure 4 is a simplified piping and instrumentation diagram (P&ID) of the experimental setup (one of the four in Figure 3). First consider the piping system (disregarding the control elements) which is designed for an ebb-and-flow (flood-and-drain) liquid mechanism: P4 pumps the nutrient solution from the reservoir up to the plant vessel elevated above the reservoir. The nutrient solution flows freely from the plant vessel through the sand filter and back down into the reservoir via the “free drain”. The pump flowrate is larger than that of the “free drain” and thus the plant vessel remains flooded while the pump is on. The excess flow from the pump (P4) returns to the reservoir via the “overflow” connection. When P4 is switched off, the plant vessel drains. P4 is switched on for 25 min and switched off for 5 min continuously, which induces the flood-and-drain mechanism.

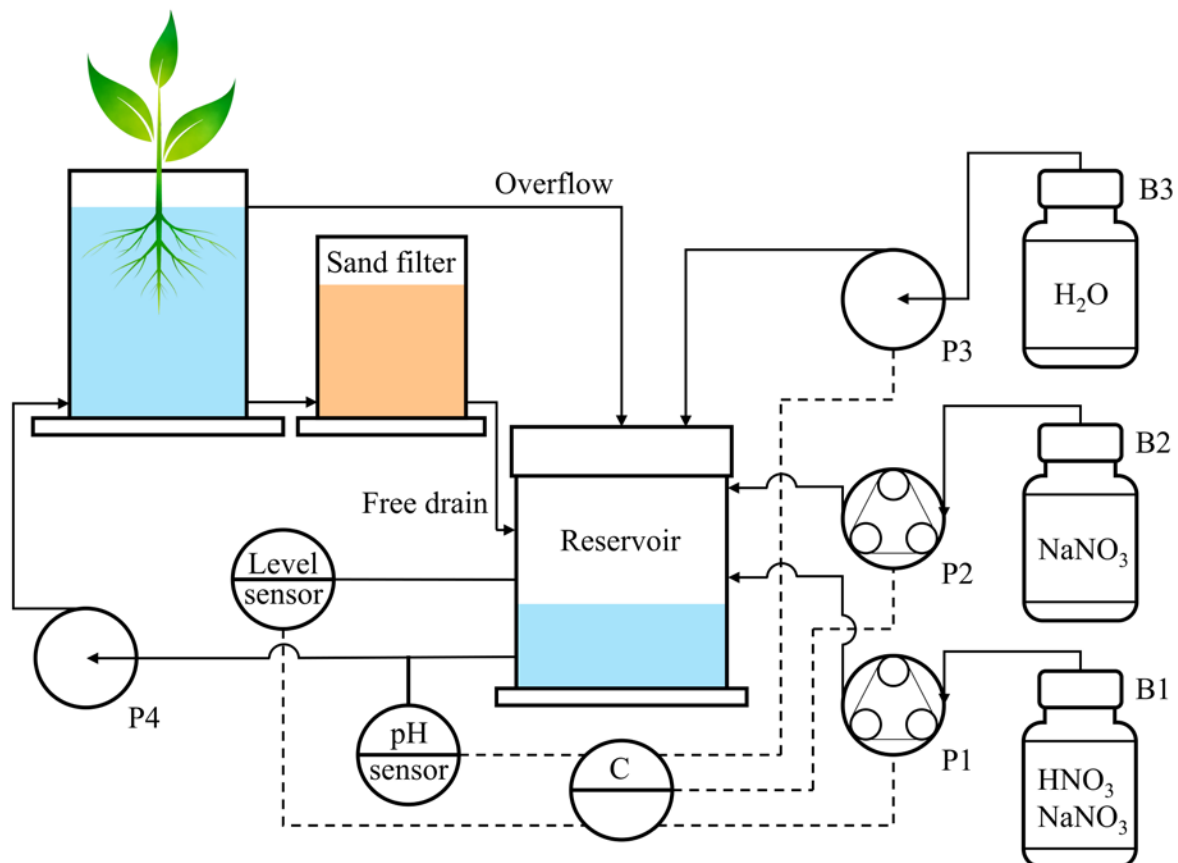


Figure 4. Simplified process flow and instrumentation diagram of the setup showing major control elements, vessels, and dosing bottles.

3.2 Method and planning

To control the nitrate concentration using pH measurements, a relationship between nitrate uptake and the change in pH of the solution had to be established. To accomplish this, run 1 was performed under standard hydroponic conditions (details given below). Nitrate absorption was measured via analysis of liquid samples and the pH was measured online and simultaneously controlled at a set-point by automatic HCl dosing. Analysis of the results yielded a functional relationship between the pH characteristics of the plants (specifically the HCl dosing rates) and nitrate absorbed during growth. Subsequently, a nitrate feed strategy was developed, which feeds nitrate at the same rate at which the plants absorb nitrate, thus achieving nitrate concentration control. This strategy was investigated in runs 2 to 4, in which the nitrate concentration was controlled at various levels. To safeguard against nitrogen depletion, which may result from errors in the predicted nitrate absorption rates, an additional control strategy was incorporated where nitrate extinction was inferred from a reduction in ∇pH (see Nomenclature). Upon nitrate extinction, the controller could immediately supply additional nitrate. The combination of the two control schemes was investigated in run 5.

In run 1, plants were cultivated in modified Hoagland's solution composed of deionised water with 5 mM KNO_3 , 5 mM $\text{Ca}(\text{NO}_3)_2 \cdot 4\text{H}_2\text{O}$, 1 mM KH_2PO_4 , 2 mM $\text{MgSO}_4 \cdot 7\text{H}_2\text{O}$, 6 mg L^{-1} NaOH, 7.5 mg L^{-1} Fe-EDTA, 0.05 mg L^{-1} Cu-EDTA, 2.9 mg L^{-1} H_3BO_3 , 1.8 mg L^{-1} $\text{MnCl}_2 \cdot 4\text{H}_2\text{O}$, 0.2 mg L^{-1} $\text{ZnSO}_4 \cdot 7\text{H}_2\text{O}$ and 0.1 mg L^{-1} $\text{Na}_2\text{MoO}_4 \cdot 2\text{H}_2\text{O}$. The solution was replaced regularly to maintain a solution strength $> 2/3$ full Hoagland's solution. The pH was controlled using 1 M HCl. In runs 2 to 5, a nitrogen-free (except for EDTA) solution was used, composed of deionised water with 2 mM K_2SO_4 , 4 mM $\text{CaCl}_2 \cdot 2\text{H}_2\text{O}$, 1 mM KH_2PO_4 , 2 mM $\text{MgSO}_4 \cdot 7\text{H}_2\text{O}$, 6 mg L^{-1} NaOH, 7.5 mg L^{-1} Fe-EDTA, 0.05 mg L^{-1} Cu-EDTA,

2.9 mg L⁻¹ H₃BO₃, 1.8 mg L⁻¹ MnCl₂·4H₂O, 0.2 mg L⁻¹ ZnSO₄·7H₂O and 0.1 mg L⁻¹ Na₂MoO₄·2H₂O. Subsequently, the desired amount of nitrate was added as KNO₃.

In runs 2, 3 and 4, the nitrate concentration was controlled by controlling the pH with a mixture of 0.3 M HNO₃ and 0.2 M NaNO₃ (composition based on the results from run 1), instead of HCl. Small amounts of NaNO₃ were added manually during runs 3 and 4 to prevent nitrate depletion. In run 5, no nitrate was added manually; instead, an automatic nitrate addition strategy was incorporated, where nitrate extinction was inferred from a reduction in ∇pH , the logistics of which are outlined in Figure 5 and explained in more detail in Section 4. The pH was controlled using 0.3 M HNO₃ only ($\alpha = 1$) to allow for a faster depletion rate of nitrate as compared with runs 2 to 4.

Seedlings were cultivated in separate systems (aeroponic cloners) and were transplanted to the main experimental setup when they weighed around 10 g, followed by commencement of the respective run. Seedlings were selected randomly in part, with preference given to visually large and healthy plants. Run 1 was conducted for a period of 21 days with solution replacement on days 7, 13, 17 and 19. Runs 2 to 4 were conducted for 13 days with solution replacement on days 5, 9 and 11. Run 5 was conducted for 11 days with solution replacement on day 7. In run 5, an initial nitrate concentration of 5 mM was charged. Nitrate extinction did not occur until after the solution had been replaced on day 7 with a nitrate concentration of 0.5 mM. A day/night cycle was implemented with 20 h light and 4 h dark in all runs except run 5, where 24 h light was employed to avoid fluctuations in ∇pH . The average relative humidity and temperature in the laboratory was maintained at 36% ($\sigma = 6\%$, $n = 570$) and 21.6 °C ($\sigma = 1.1$ °C, $n = 570$). In all runs, the nitrate concentration was measured via spectrophotometric analysis of liquid samples. Relative leaf chlorophyll content was measured by

dissolving dry leaf material in acetone (2.44 g L^{-1}) and measuring the absorbance at 663 nm. No absolute quantification of chlorophyll content was done, thus only a reduction in chlorophyll content could be detected. Plants were dried at $70 \text{ }^\circ\text{C}$ for 48 hours.

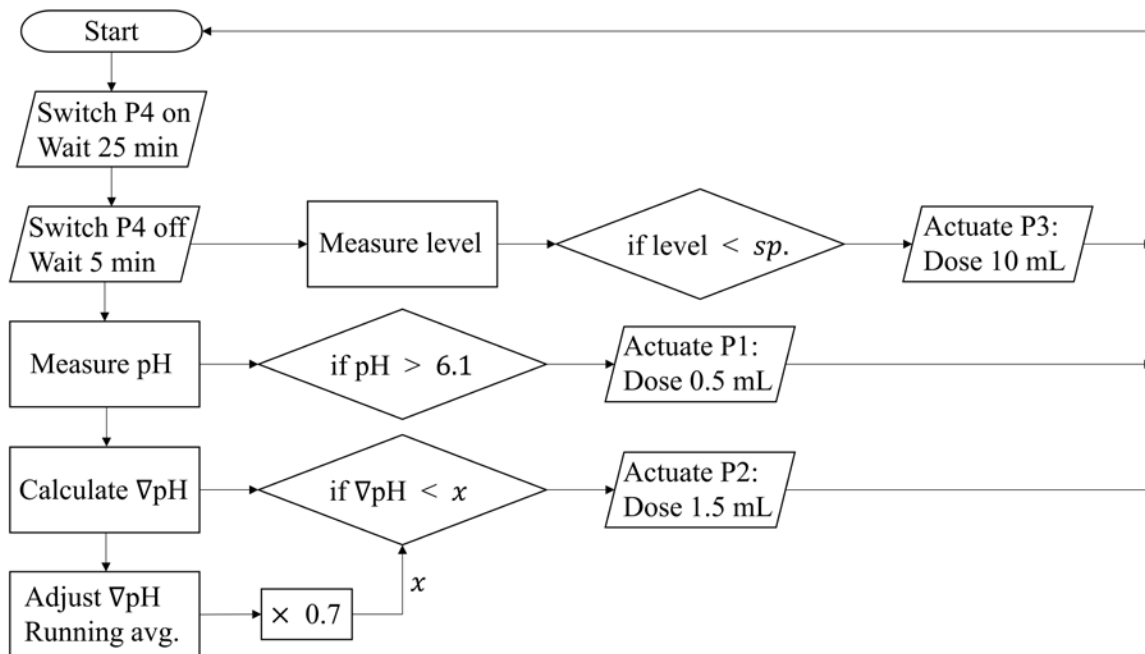


Figure 5. Sequential function chart of the control algorithm responsible for the flood-and-drain mechanism (switching P4 on and off), liquid level control (first horizontal branch), pH control (second branch) and nitrate extinction prevention (bottom branch). The bottom two branches were implemented in run 5 only. “*sp.*” corresponds to a set point of 1.8 L.

3.3. Apparatus and instruments

A single Arduino Mega 2560™ was used to control the water level, pH, and flood-and-drain mechanism in all four systems. Gravity™ pH probes (HAOSHI™ pH meter Pro) were used for online pH measurements. Generic™ peristaltic pumps (Precision Peristaltic Pump + Intelligent Stepper Controller)

were used for dosing. All chemicals/nutrients were purchased from Merck™ (BioXtra®, ≥ 99.0%). For plant lighting, 4 x Mars Hydro™ 400 W blue/red LED lights (Mars II 400 LED Grow Light®) were used. Kale seeds (*Brassica oleracea* var. *sabellica* or Vate's Blue Curled Kale) were purchased from Raw™. The main pumps (responsible for the flood-and-drain mechanism) were purchased from Xylem™ (Flojet Diaphragm Electric Operated Positive Displacement Pump, 3.8 L min⁻¹, 2.5 bar, 12 V DC). For seedling propagation, aeroponic systems (Aeroponic Cloner) purchased from hydroponic.co.za™ were used. Nitrate concentration was measured in a spectrophotometer (Agilent Technologies™, Cary 60 UV-Vis, G6860A) using Merck™ Nitrate Cell Test, DMP 23 - 225 mg/L NO₃-N and DMP 0.10 - 25.0 mg/L NO₃-N Spectroquant®. Relative chlorophyll content was determined using pure acetone (99.99%), purchased from Promark Chemicals™.

4. Results and discussion

4.1 Relating nitrate absorption to proton dosing

To establish the relationship between nitrate absorption and proton dosing, run 1 was performed using standard Hoagland's solution (high nitrate concentration). The results from the 21-day run are given in Figure 6 in which the proton dosing, nitrate absorption and transpiration rates of the four separate runs are plotted against time. The pH was controlled at an average value of 6.05 ($\sigma = 0.07$, $n = 997$). The exponential nature of the plots suggests that the setup allows for population growth characteristics (Hellgren, 1996; Raistrick, 1999). Figure 6 (c) shows a plot of the HCl dosing rates vs. the nitrate absorption rates using the data from Figure 6 (a) and (b), which indicates a constant ratio of proton dosing required for pH homeostasis and nitrate absorbed by the plant ($\eta \approx 0.49$ mol mol⁻¹). Thus, for every mol of nitrate absorbed, approximately 0.49 mols of protons were dosed to maintain the solution's pH. This relationship provides the means of inferring the nitrate absorption rate from the proton dosing rate.

To control the nitrate concentration, nitrate must be fed at the same rate at which the plants absorb nitrate. Provided that for every mol of nitrate absorbed, 0.49 mols of protons need to be dosed to maintain the solution's pH, the required nitrate feed rate is 1/0.49 of the proton dosing rate. Instead of incorporating a separate nitrate feed system, a simpler technique was employed, where the acid dosing solution (B1 in Figure 4) was composed of a proton to nitrate ratio of 0.49 ($\alpha = \eta = 0.49$). Thus, by controlling the pH with the acid-nitrate dosing solution, the nitrate concentration will be controlled simultaneously. Runs 2, 3 and 4 employed this strategy to control the nitrate concentration at 11 mM, 1 mM, and 0.5 mM.

4.2 Controlling pH and nitrate concentration simultaneously using a single dosing reservoir.

It was observed in trial experiments (not reported) that an α value of 0.5 mol mol⁻¹ resulted in slow accumulation of nitrate in solution, whereas an α value of 0.6 resulted in slow depletion of nitrate. Inevitable variation in η , due to genetics or changes in plant growth stage, or variation in α due to error in composing the acid dosing solution (B1 in Figure 4), will result in either accumulation or depletion of nitrate in solution. Thus, conceding that α will not equal η exactly, an α value of 0.6 mol mol⁻¹ (allowing for slow depletion of nitrate in solution) was employed in runs 2, 3 and 4. Nitrate depletion was prevented by small manual additions of NaNO₃ in runs 3 and 4.

Figure 7 (a) to (c) gives the nitrate concentrations (marked as triangles with magnitudes on the left vertical axis) for runs 2 to 4, respectively. Vertical dotted lines indicate the times at which the solution was replaced. A common/bulk dosing solution (B1 in Figure 4) was used in all three runs. Thus, variation in the rate of nitrate depletion in solution is due to variation in η , as α remained constant. Relatively constant nitrate concentration profiles are observed. For run 2, with an initial nitrate concentration of 11.5 mM, no additional nitrate was added manually. A slight decrease in nitrate concentration can be observed between solution replacements, indicating that the choice of α is larger than the plant's η value. In runs 3 and 4, additional nitrate was added manually to correct for the gradual decrease in concentration. Manually added amounts are plotted as bars in Figure 7 with magnitudes on the right vertical axis. Given the manual additions as well as the quantified automatic dosages of acid and nitrate, the total nitrate consumed could be calculated. It was found that manual dosing accounted for 8%

($\sigma = 4$, $n = 8$) of the total nitrate addition. The calculated η values varied between 0.52 and 0.57, with an average value of 0.55 for the eight plants.

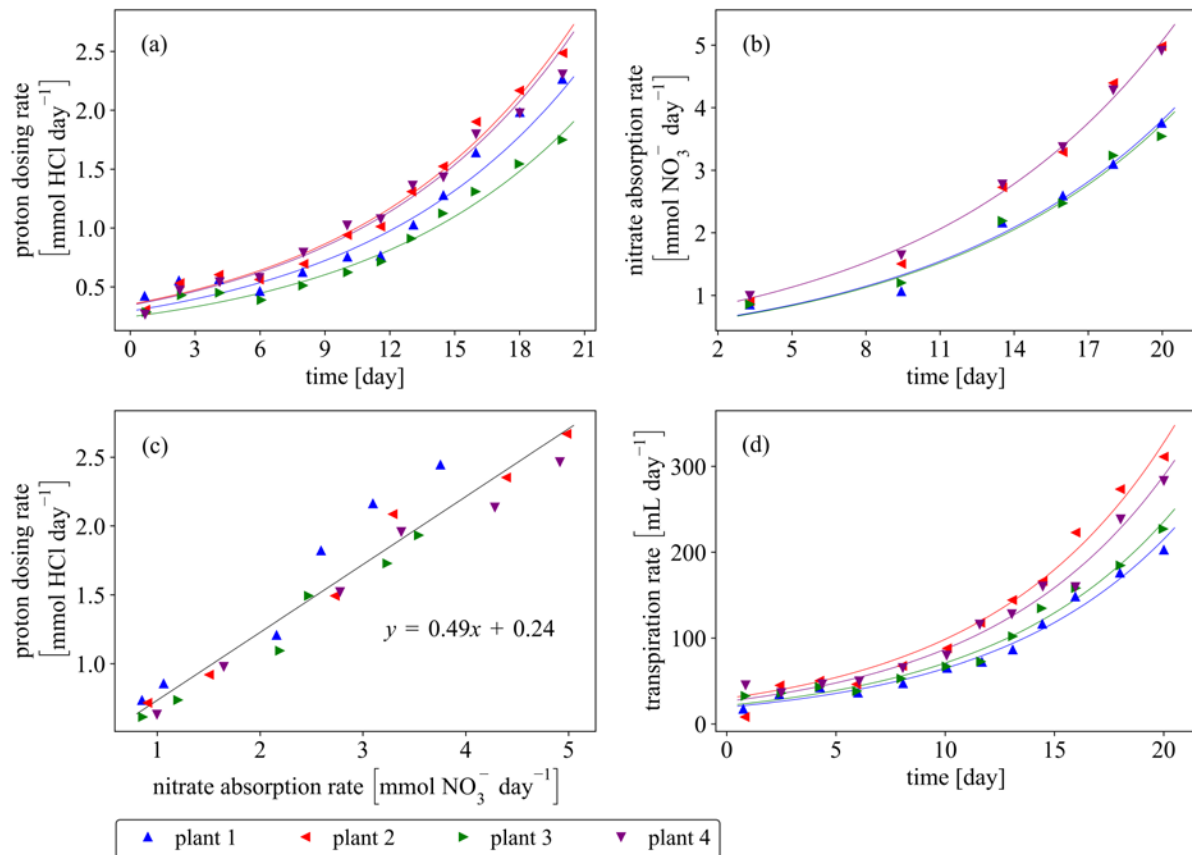


Figure 6. Results from run 1 using Hoagland’s solution with frequent replacement (average nitrate concentration of 12 mM). The pH was controlled at an average value of 6.05 ($\sigma = 0.07$, $n = 997$). HCl dosing rates (a), nitrate absorption rates (b) and transpiration rates (d) all exhibit an exponential increase. Subplot (c) relates proton dosing to nitrate absorption where a fitted value of $\eta = 0.49$ is obtained.

Given that the same dosing solution was used during runs 2 to 4, from Figure 7 it can be seen that η varied between plants. For example, in run 3, the plant cultivated in system 2 (plant 2) had the lowest η value (as more nitrate had to be added manually), whereas in run 4, plant 1 had the lowest η value. Thus, it is clear that η varies slightly between plants, which may be due to genetic differences in nutrient uptake characteristics.

Figure 8 (a), (b) and (c) provide the proton-nitrate dosing rates (D_R) for runs 2 to 4 where the natural logarithm is used to linearise the growth curves. The linear trends resulting from the logarithmic plots indicate exponential growth characteristics, as observed in run 1. It can be shown from the population growth equation that the slopes of the fitted lines equal the relative dosing rates (RDR) (Hellgren, 1996; Raistrick, 1999). Practically identical relative dosing rates are observed, which are in agreement with the relative growth rates (RGR , fresh mass based) given in Figure 8 (d). Thus, it is evident that no reduction in growth rate occurred with decreasing nitrate concentration. To the contrary, there appears to be a slight increase in the growth parameters.

Figure 8 (d) compares the average growth parameters (RGR and RDR) of the three runs reported in Figure 8 (a) to (c). It is evident that the relative growth rates (RGR) are higher than the relative dosing rates (RDR), which indicates that less nitrogen per plant mass is absorbed with increasing plant size. This can be attributed to a decreasing η value with plant size (fewer protons need to be dosed to maintain the pH at the same nitrate absorption rate). However, no further evidence of this has been found in the data. Instead, it is assumed that the nitrogen content in the plants decreases with plant size, which is corroborated by Le Bot et al. (1998).

Assuming that nutrients are absorbed in constant ratios relative to one another, i.e. constant biomass composition, all nutrients may potentially be controlled in the same manner as nitrate. For example, if potassium is absorbed at half the rate of nitrogen absorption, a potassium to nitrate ratio in the acid dosing bottle of 0.5 mol mol⁻¹ will control the potassium concentration equally well.

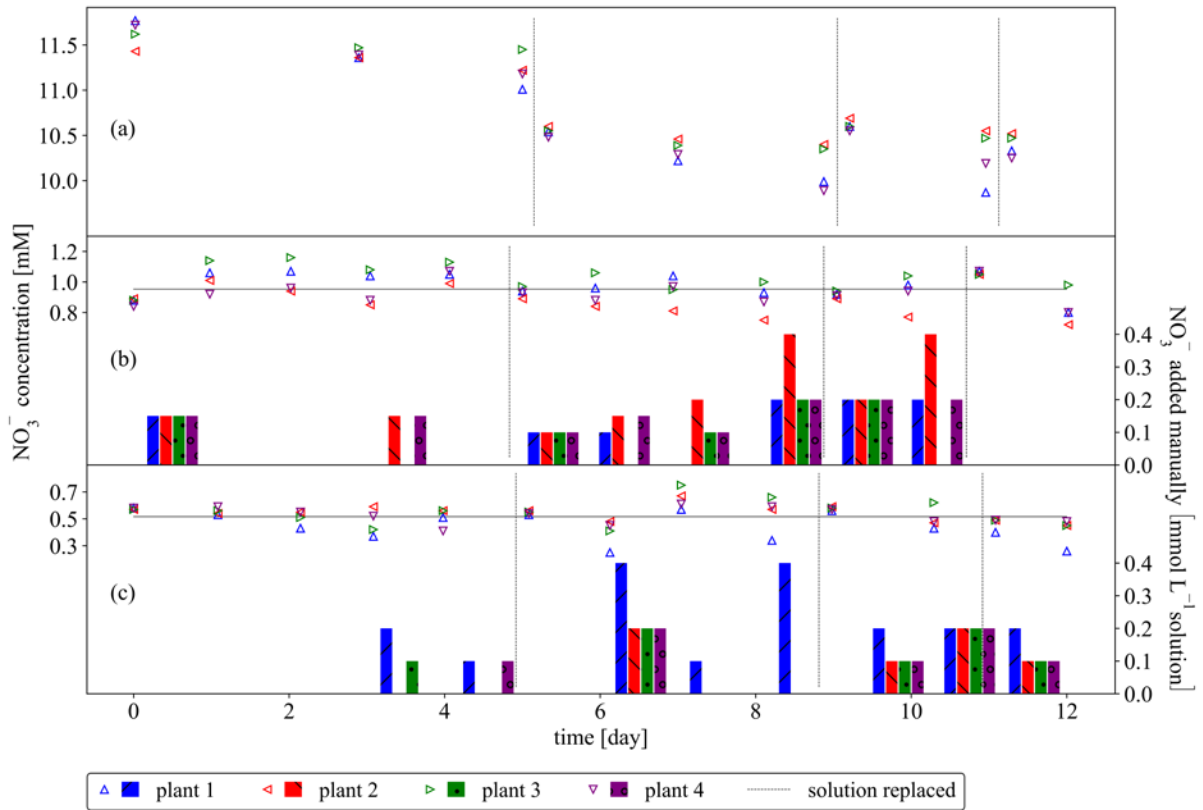


Figure 7. Results from runs 2 to 4. Nitrate controlled at approximately 1 and 0.5 mM for runs 3 and 4, respectively. All runs used the same dosing solution composed of 0.3 M HNO_3 and 0.2 M NaNO_3 ($\alpha = 0.6 \text{ mol mol}^{-1}$). For runs 3 and 4 manual corrections were made with NaNO_3 as indicated by bar plots in (b) and (c). Vertical dotted lines indicate solution replacement.

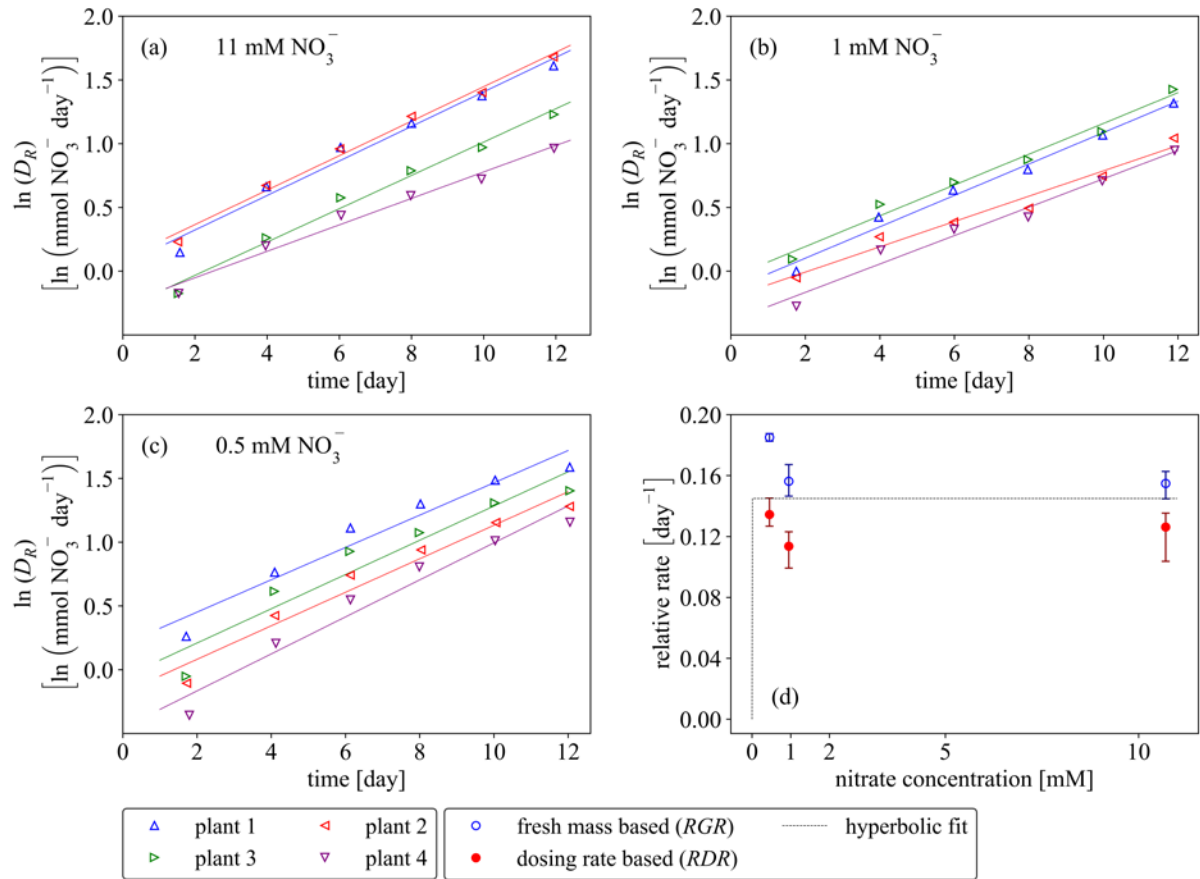


Figure 8. Subplots (a), (b) and (c) provide logarithmic plots of the dosing rates (D_R) for runs 2 to 4. The slopes of the fitted lines equal the RDR values. Subplot (d) gives RDR and RGR as a function of the nitrate operating concentration. Error bars span the data range (min. \leftrightarrow max.) of the four plants.

4.3 Automatic prevention of nitrate depletion using a second dosing reservoir.

For run 5, nitrate addition was fully automated (no manual addition). In addition to the nitrate-control strategy used in runs 2 to 4, where the nitrate concentration was controlled by controlling the pH with a mixture of acid and nitrate (such that $\alpha \approx \eta$), a second dosing pump (P2 in Figure 4) and a dosing solution containing NaNO_3 only (B2 in Figure 4) was installed, the purpose of which was to dose

automatically the extra required nitrate which previously had to be added manually in runs 3 and 4 to prevent nitrate depletion.

It was noted in trial experiments that ∇pH decreased as the nitrate concentration approached zero. This can most likely be attributed to a reduction in the nitrate assimilation rate when nitrate concentrations are critically low. Thus, nitrate extinction may be inferred from a reduction in ∇pH , which upon detection, can actuate the second dosing pump P2, as outlined in Figure 5. The extra nitrate will then only be added upon extinction of nitrate in the solution. Provided that the nitrate concentrations are not critically low for any significant period, this strategy should satisfy the plant's nitrogen demands while maintaining low nitrogen concentrations. The results from the last four days of the run are given in Figure 9 (no nitrate extinction occurred prior to this), which shows how ∇pH decreases when nitrate becomes extinct. This is conveyed by plotting the nitrate concentrations together with the relative ∇pH measurements. The relative ∇pH measurements are the ratios of the instantaneous ∇pH measurements to the running average of the ∇pH measurements (average over the past 6 hours). As described in Figure 5, the controller doses additional nitrate when this ratio falls below 0.7, indicating a 70% reduction in ∇pH . Consistent dosing occurring approximately every 6 hours is observed, which suggests that the strategy works well to provide the extra required nitrogen which previously had to be added manually in runs 3 and 4. Furthermore, a favourably fast response is observed where an increase in ∇pH (recovery) is apparent immediately after dosing. As shown in Figure 9, the nitrate concentrations varied between 0 and 0.2 mM, which is two orders of magnitude lower than the standard protocol.

In Figure 10, the average *RGR* and *RDR* values for run 5 are given in the top right-hand box. For comparison, the average *RGR* and *RDR* values for runs 2 to 4 (total of 12 plants) are given in the top left-hand box. Similar growth rates are

observed between run 5 and runs 2 to 4, considering that the plants in run 5 received 20% more light (no night cycle to prevent fluctuations in ∇pH). The root mass fraction and relative chlorophyll content for each of the four runs are plotted as bars, with relative chlorophyll content on the left vertical axis and root mass fraction on the right vertical axis. A slight increase in root mass fraction and leaf chlorophyll content with decreasing nitrate concentration is observed.

The results provide clear evidence that plant growth is not sacrificed when operating at the nitrate concentrations investigated. The results also give a preliminary indication that plant nutrition was not affected. With regard to nitrogen spillage, the results are very promising since the effluent from the hydroponic unit contains a nitrate level two orders of magnitude lower than in conventional operation. This implies that the load of nitrates dumped into the environment can be drastically reduced without sacrificing crop growth and nutrition.

It should be mentioned that the water used in commercial hydroponic systems often contain alkaline species such as carbonates (found in tap water, for example). The experiments were performed using deionized water and thus changes in pH were caused solely by the plants. Other changes in pH not caused by the plants would need to be accounted for or removed when implementing this strategy.

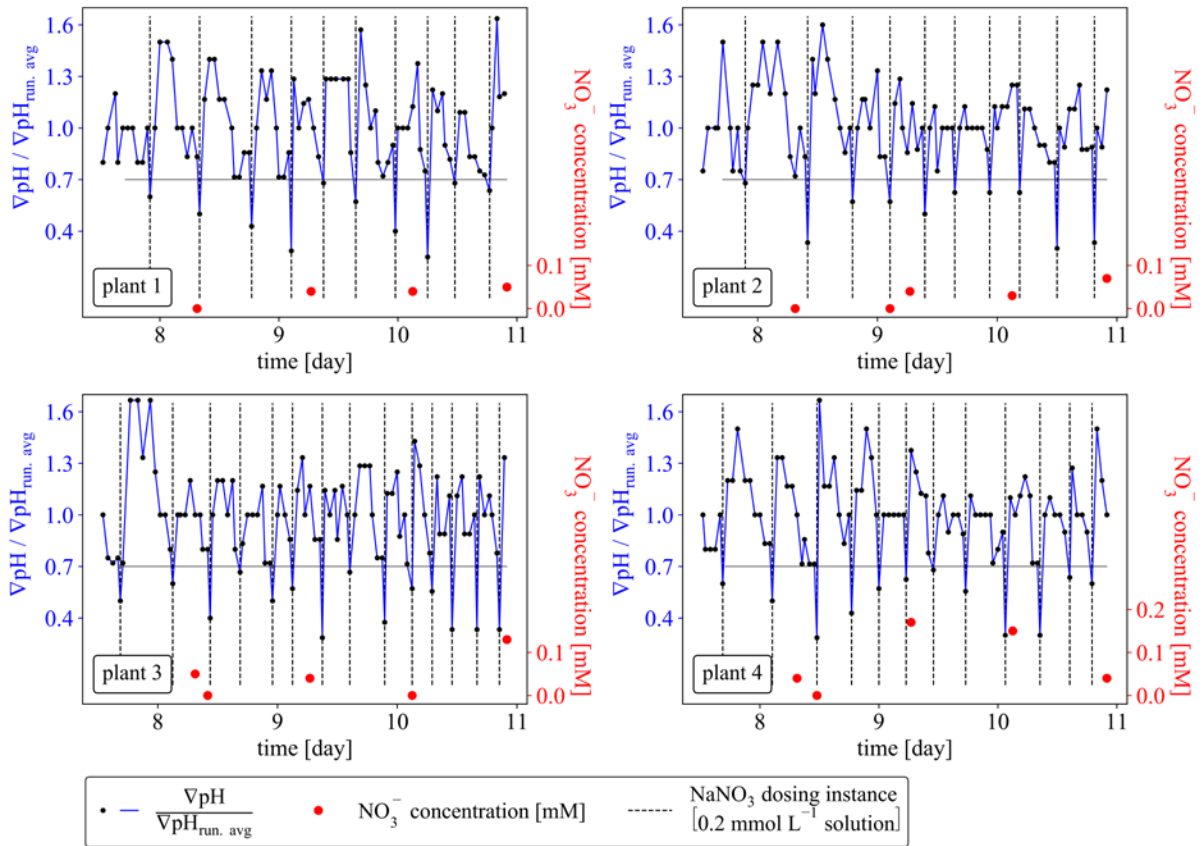


Figure 9. Results from run 5. Shown are profiles of ∇pH divided by the running average of ∇pH . As described in Figure 5, NaNO_3 dosing (from B2 in Figure 4) occurs when there is a 70% reduction in ∇pH , whereupon $0.2 \text{ mmol NaNO}_3 \text{ L}^{-1}$ solution is dosed. Also shown, are the measured nitrate concentrations in solution.

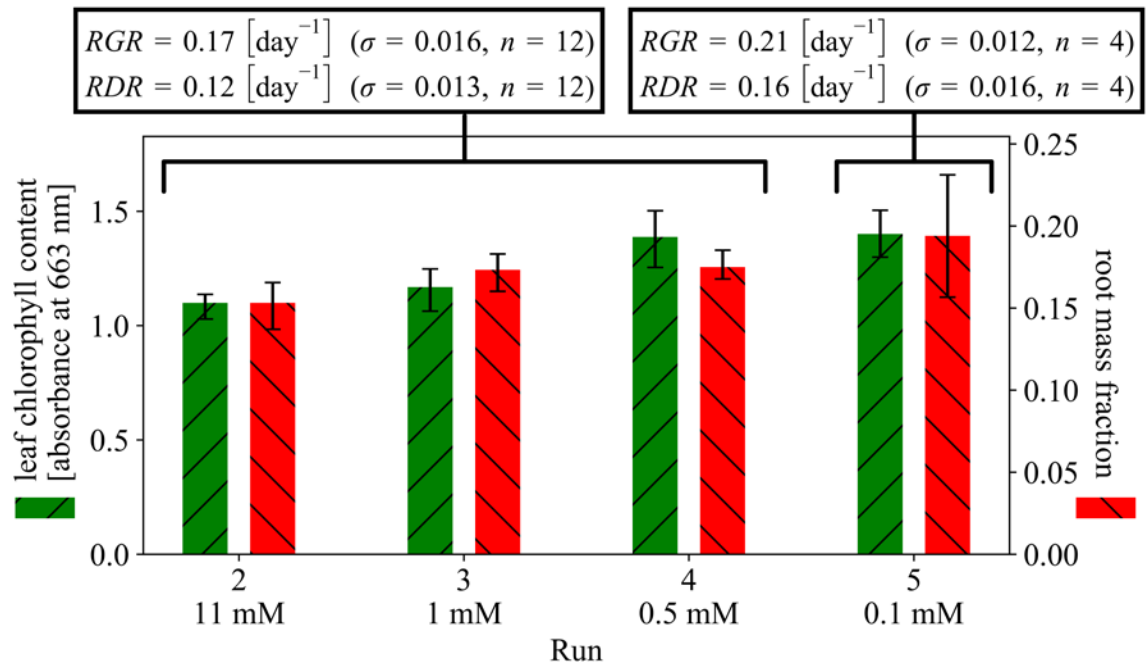


Figure 10. Comparison of leaf chlorophyll content and root mass fraction of runs 2 to 5. Also shown are average values of the growth parameters RGR and RDR for runs 2 to 4, which are compared against the growth parameters for run 5 (20% more light was received) in two separate annotations. Error bars span the data range (min. \leftrightarrow max.) of the four plants.

5. Conclusions

It was shown that the nitrate concentration in a hydroponic system can be controlled at much lower levels compared with the standard protocol using pH as the sole measured variable, without sacrificing plant health or growth rate. This was accomplished by selecting an α value slightly higher than the plant's η value, which allows for a slow depletion rate of nitrate in solution. As depletion ultimately results in extinction, an automatic nitrate-addition strategy was included where nitrate extinction was inferred from a reduction in the rate of change of pH. This combination was successful at maintaining nitrate concentrations below 0.2 mM without sacrificing plant health or growth rate. A cheap and simple control strategy was developed to reduce nitrogen spillage to the environment. The control scheme can easily be incorporated into commercial hydroponic farms where pH measurement and control are standard.

From an environmental perspective, the suggested control strategy has the potential to reduce nitrate pollution into the hydrosphere. The fast-growing soilless agriculture sector has the potential to become a noteworthy contributor to nutrient spillage into waterways, and circumventing design strategies are required to reduce environmental harm. The control scheme presented here can easily be incorporated into commercial hydroponic farms where pH measurement and control are standard procedures and thus it provides an achievable strategy for reducing nitrogen pollution.

References

Andersen L. J., Kristiansen H., 1983. Nitrate in groundwater and surface water related to land use in the Karup Basin, Denmark. *Env. Geo.* 4, 207-212.

<https://doi.org/10.1007/BF02414865>

Arnon, D. I., Hoagland, D. R., 1940. Crop production in artificial culture solutions and in soils with special reference to factors controlling yields and absorption of inorganic nutrients. *Soil Sci.*, 50, 463–485.

Bijay-Singh, Yadvinder-Singh, Sekhon, G. S., 1995. Fertilizer-N use efficiency and nitrate pollution of groundwater in developing countries. *J. Cont. Hydro.* 3, 167-184. [https://doi.org/10.1016/0169-7722\(95\)00067-4](https://doi.org/10.1016/0169-7722(95)00067-4)

Bugbee, B., 2004 Nutrient management in recirculating hydroponic culture. *Acta Horticulturae*, 648, 99–112.

Burris, R. H., 2001. Nitrogen fixation. University of Wisconsin-Madison, Madison, Wisconsin, USA

Chao, W., Pei Fang W., 2008. Migration of infiltrated NH_4 and NO_3 in a soil and groundwater system simulated by a soil tank project supported by the National Key Basic Research Program (973 program) of China (No. 2002CB412303), the National Natural Science Foundation of China (No. 50709009), and the key project of Chinese Ministry of Education (No. 106088). *Pedosphere*. 5, 628-637.

Chen D., Suter H., Islam A., Edis R., Freney J. R., Walker C. N., 2008. Prospects of improving efficiency of fertiliser nitrogen in Australian agriculture: a review of enhanced efficiency fertilisers. *Australian J. of Soil Res.* 46, 289-301. <https://doi.org/10.1071/SR07197>

Cho, W. J., Kim, H. J., Jung, D. H., Kim, D. W., Ahn, T. I., Son, J. E., 2018. On-site ion monitoring system for precision hydroponic nutrient management. *Comp. Electron. Agr.*, 146, 51–58. <https://doi.org/10.1016/j.compag.2018.01.019>

Christie E., 2014. Water and nutrient reuse within closed hydroponic systems. PhD thesis, Georgia Southern University.

Cooper, A., 1988. “1. The system. 2. Operation of the system”. In: *Grower Books (Ed.), The ABC of NFT. Nutrient Film Technique*, 3-123, Nexus Media, London.

del Amor, F. M., Porras, I., 2009. Effects of plantgrowth-promoting bacteria on growth and yield of pepper under limited nitrogen supply. *Can. J. Plant Sci.*, 89(2), 349–358. <https://doi.org/10.4141/CJPS08116>

Delgado, J.A., 2002. Quantifying the loss mechanisms of nitrogen. *J. Soil Water Conserv.* 57, 389-398.

Dijkshoorn, W., 1962. Metabolic regulation of the alkaline effect of nitrate utilization in plants. *Nature*, 194, 165-167. <https://doi.org/10.1038/194165a0>

Domingues, D. S., Takahashi, H. W., Camara, C. A. P., Nixdorf, S. L., 2012. Automated system developed to control pH and concentration of nutrient

solution evaluated in hydroponic lettuce production. *Comp. Electron. Agr.*, 84, 53-61. <https://doi.org/10.1016/j.compag.2012.02.006>

Eickhout, B., Bouwman, A.F., van Zeijts, H., 2006. The role of nitrogen in world food production and environmental sustainability. *Agric. Ecosyst. Environ.* 116, 4-14. <https://doi.org/10.1016/j.agee.2006.03.009>

Erismann, J.W., Sutton, M.A., Galloway, J., Klimont, Z., Winiwarter, W., 2008, How a century of ammonia synthesis changed the world. *Nat. Geosci.*, 1, 636-639

Goins, G., Yorio, N., Wheeler, R., 2004. Influence of nitrogen nutrition management on biomass partitioning and nitrogen use efficiency indices in hydroponically grown potato. *J. Amer. Soc. Hort. Sci.*, 129(1), 134-140. <https://doi.org/10.21273/JASHS.129.1.0134>

Gustafson, A., 1983. Leaching of nitrate from arable land into groundwater in Sweden. *Env. Geo.* 2, 65-71. <https://doi.org/10.1007/BF02381098>

Hellgren, O., Ingestad, T., 1996. A comparison between methods used to control nutrient supply. *J. Exp. Bot.*, 47(1), 117–122. <https://doi.org/10.1093/jxb/47.1.117>

Hewitt, E. J., 1996. Sand and water culture methods used in the study of plant nutrition. Technical Communication No. 22. Commonwealth Bureau of Horticulture and Plantation Crops, East Malling, Maidstone, Kent, England.

Hosseinzadeh, S., Verheust, Y., Bonarrigo, G., Van Hulle. S., 2017. Closed hydroponic systems: operational parameters, root exudates occurrence and related water treatment, *Rev Environ Sci Biotechnol* 16, 59–79.

<https://doi.org/10.1007/s11157-016-9418-6>

Imsande, J., 1986. Nitrate-ammonium ratio required for pH homeostasis in hydroponically grown soybean. *J. Exp. Bot.*, 37(3), 341–347.

<https://doi.org/10.1093/jxb/37.3.341>

Isermann, K., 1990. Share of nitrogen and phosphorus emissions into the surface water of W. Europe against the background of their eutrophication. *Fertiliser Res.* 26, 253-269.

Kanter, D.R., Bartolini, F., Kugelberg, S., Leip, A., Oenema, O., Uwizeye, A., 2020. Nitrogen pollution policy beyond the farm. *Nat. Food*, 1, 27–32.

<https://doi.org/10.1038/s43016-019-0001-5>

Kim, H. J., Kim, W. K., Roh, M. Y., Kang, C. I., Park, J. M., Sudduth, K. A., 2013. Automated sensing of hydroponic macronutrients using a computer controlled system with an array of ion-selective electrodes. *Comp. Electron. Agr.*, 93, 46–54. <https://doi.org/10.1016/j.compag.2013.01.011>

Kumar, R. R., Cho, J. Y., 2014. Reuse of hydroponic waste solution. *Env. Sci. Poll. Res.*, 21(16), 9569–9577. <https://doi.org/10.1007/s11356-014-3024-3>

Kuzyakov, Y., Xu, X., 2013. Competition between roots and microorganisms for nitrogen: mechanisms and ecological relevance, *New Phytologist*, 198: 656–669. <https://doi.org/10.1111/nph.12235>

Le Bot, J., Adamowicz, S., Robin, P., 1998. Modelling plant nutrition of horticultural crops: a review, *Scientia Horticulturae*, 74 (1–2), 47–82.

[https://doi.org/10.1016/S0304-4238\(98\)00082-X](https://doi.org/10.1016/S0304-4238(98)00082-X)

Le Deunff, E., Malagoli, P., Decau, M.-L., 2019. Modelling nitrogen uptake in plants and phytoplankton: advantages of integrating flexibility into the spatial and temporal dynamics of nitrate absorption. *Agronomy*, 9 (3), 116.

<https://doi.org/10.3390/agronomy9030116>

Lenord Melvix, J. S. M., Sridevi, C., 2014. Design of efficient hydroponic nutrient solution control system using soft computing based solution grading. Proceedings of the 2014 International Conference on Computation of Power, Energy, Information and Communication, ICCPEIC 2014, p 148–154.

<https://doi.org/10.1109/ICCPEIC.2014.6915356>

Li, J. H., Yang, X. Y., Wang, Z. F., Shan, Y., Zheng, Y., 2015. Comparison of four aquatic plant treatment systems for nutrient removal from eutrophied water. *Bioresour. Technol.*, 179, 1-7.

<https://doi.org/10.1016/j.biortech.2014.11.053>

Mathias, M., 2014. Emerging Hydroponics Industry. *Pract. Hydroponics Greenhouses*, 144, 18.

Miles, A., Burris, R., Evans, H., Stacey, G., 1992. Biological nitrogen fixation, Chapman & Hall, New York.

Miller A., Adhikari R., Nemali K., 2020. Recycling nutrient solution can reduce growth due to nutrient deficiencies in hydroponic production. *Front. Plant. Sci.*, <https://doi.org/10.3389/fpls.2020.607643>

Prystay, W., Lo, K. V., 2001. Treatment of greenhouse wastewater using constructed wetlands. *J. Environ. Sci. Health B*, 36, 341–353. <https://doi.org/10.1081/PFC-100103574>

Raistrick, N., 1999. An automated relative-addition rate nutrient-dosing system for use in flowing solution culture. *J. Exp. Bot.* 50, (331), 263-267. <https://doi.org/10.1093/JXB/50.331.263>

Raven, J. A., Smith, F. A., 1976. Nitrogen assimilation and transport in vascular land plants in relation to intracellular pH regulation. *New Phytologist*, 3, 415-431. <https://doi.org/10.1111/j.1469-8137.1976.tb01477.x>

Rufi-Salis, M., Calvo, M. J., Petit-Boix, A., Villalba, G., Gabarrell, X., 2020. Exploring nutrient recovery from hydroponics in urban agriculture: an environmental assessment. *Resour. Conserv. Recycl.* 155, 104683. <https://doi.org/10.1016/j.resconrec.2020.104683>

Seungjun, Lee, Jiyoung, Lee, 2015. Beneficial bacteria and fungi in hydroponic systems: Types and characteristics of hydroponic food production methods, *Scientia Horticulturae*, 195, 206-215. <https://doi.org/10.1016/j.scienta.2015.09.011>

Silberbush, M., Ben-Asher, J., 2001. Simulation study of nutrient uptake by plants from soilless cultures as affected by salinity buildup and transpiration. *Plant Soil*, 233(1), 59–69. <https://doi.org/10.1023/A:1010382321883>

Smith, F. A., and Raven, J. A., 1979. Intracellular pH and its regulation. *Annu. Rev. Plant Physiol.*, 30, 289-311.

<https://doi.org/10.1146/annurev.pp.30.060179.001445>

Steiner, A. A., 1984. The universal nutrient solution. Proceedings of the 6th International Congress on Soilless Culture, Wageningen, The Netherlands, 29 Apr - 5 May, 1984, pp 633-650

Trejo-Téllez, L., Gómez-Merino, F., (2012). Nutrient solutions for hydroponic systems” Colegio de Postgraduados, Montecillo, Texcoco, State of Mexico, Mexico

Wang, B., Shen, Q., 2012. Effects of ammonium on the root architecture and nitrate uptake kinetics of two typical lettuce genotypes grown in hydroponic systems, *J. Plant Nutr.*, 35, 1497-1508.

<https://doi.org/10.1080/01904167.2012.689910>

Withers, P. J. A., Lord, E.I., 2002. Agricultural nutrient inputs to rivers and groundwaters in the UK: policy, environmental management and research needs. *Sci. Tot. Env.* 9-24, 282 - 283

Appendix

Experimental design and construction

The plant vessels (four copies) were constructed from square acrylic sheets to form the base of the vessel, acrylic tubes to form the body and smaller tubes for piping attachments. Holes were drilled into the large tube for insertion of the small tubes. The sheet and tubes were glued together with an acrylic adhesive. The vessels were spray painted until opaque to prevent algae growth. A stainless-steel mesh cylinder was inserted into the plant vessel and sand filter (also shown in Figures A2 and A3) to prevent the plant roots from interfering with the liquid flow in the plant vessel and to contain the sand in the filter. A foam collar was inserted into the mesh which served to support the plant.

The top of the reservoirs were closed with PVC female end caps. Holes were drilled into the end caps for the insertion of control components. A float switch (level sensor) to control the liquid level was fitted into the 14 mm drilled hole. Within the reservoir was a liquid inlet acrylic tube; the bottom of the tube was fitted with a cylindrical sponge to reduce splashing. An 18 mm hole was drilled into the centre of the end cap for attachment of a 10 mL pipette tip, which allowed air to move freely and prevented any droplets (splashing) from escaping.

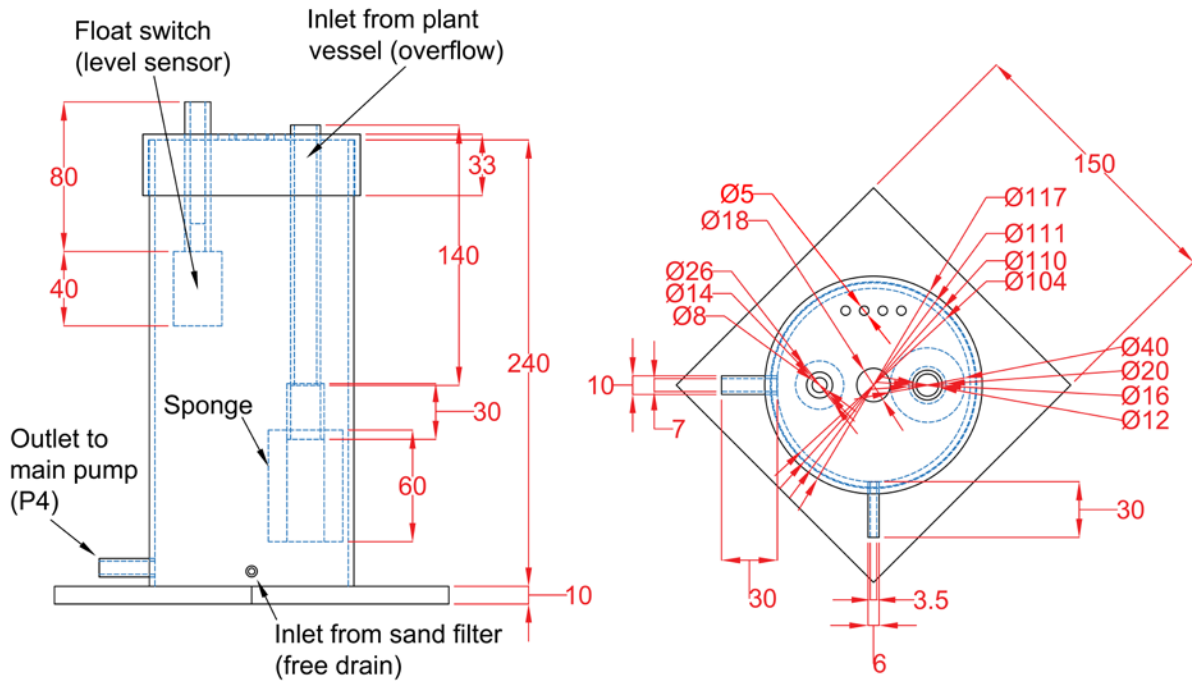


Figure A1. Detailed drawing of the nutrient solution reservoir. Side view on left, top view on right.

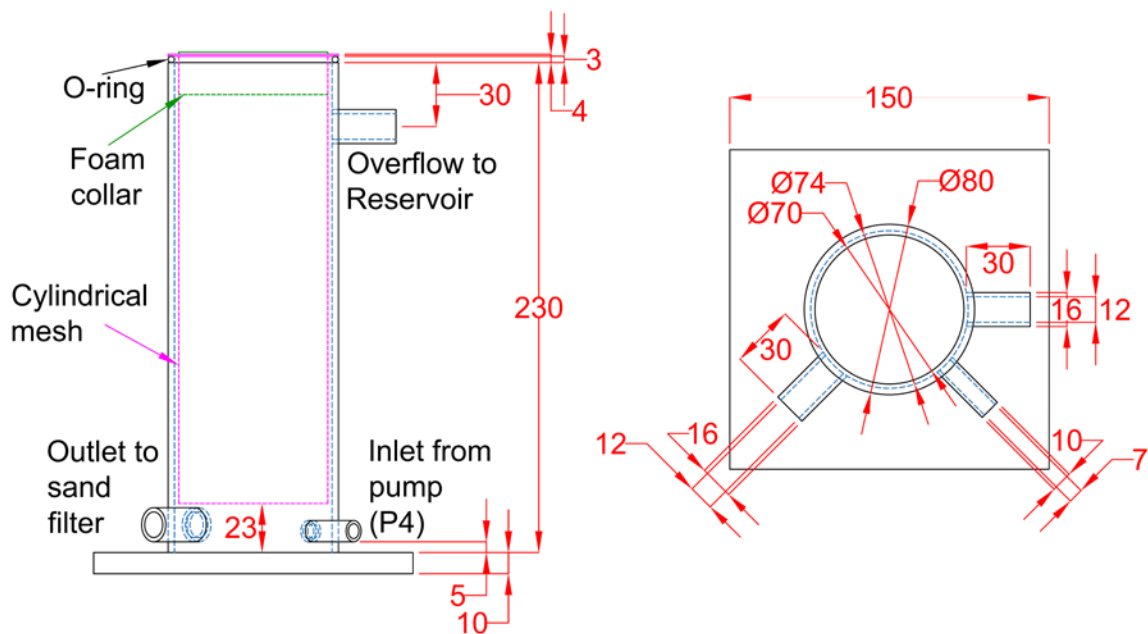


Figure A2. Detailed drawing of the plant vessel. Side view on left, top view on right.

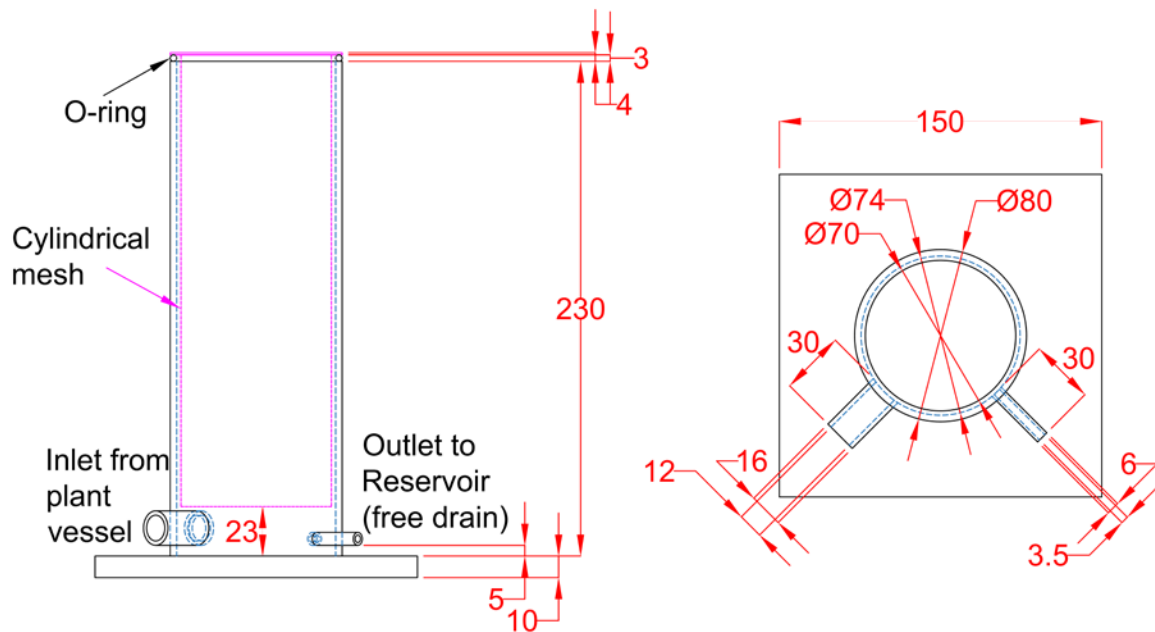


Figure A3. Detailed drawing of the sand filter. Side view on left, top view on right.

Detailed circuitry connecting the control components shown in Figure 4 is given in Figure A4. An Arduino™ was used as the controller platform, which was responsible for automation of the flood-and-drain pumps (P4 in Figure 4), online pH measurement, level control via water addition and acid/nitrate dosing.

The acrylic plastics used in the construction of the plant vessel and reservoir were purchased from Maizey's Plastics™. Acrylic adhesive, Magma Bond C1, was also purchased from Maizey's Plastics™. The opaque (black) silicone tubes for liquid transport between vessels were purchased from Uxcell™ on Amazon™. The mesh cylinders (50-micron Premium Infuser Cold Coffee Maker for 2QT Wide Mouth Mason Jars, 64 oz), used in the plant vessels, were purchased from Modern Joe's™ on Amazon™ and the 300-micron mesh filters (Beer Dry Hopper Filter, 300 Micron Mesh Stainless Steel Hop Strainer Cartridge, Homebrew Hops Beer & Tea Kettle Brew Filter) used in the sand filters were purchased from

Fashionclubs™ on Amazon™. The cloning collars (3-inch Cloning Collars Inserts Premium Grade Foam Better Than Neoprene for Hydroponics Plant Germination in DIY Cloner & Clone Machines) used for plant support were purchased from Cz Garden™ on Amazon™. The filter sponges for preventing splashing from the overflow tube into the reservoir were purchased from Powkoo™ on Amazon™. The float switches (Stainless Steel Mini Vertical Liquid Water Level Sensor Float Switch) were purchased from Lyhpccom™ on Amazon™.

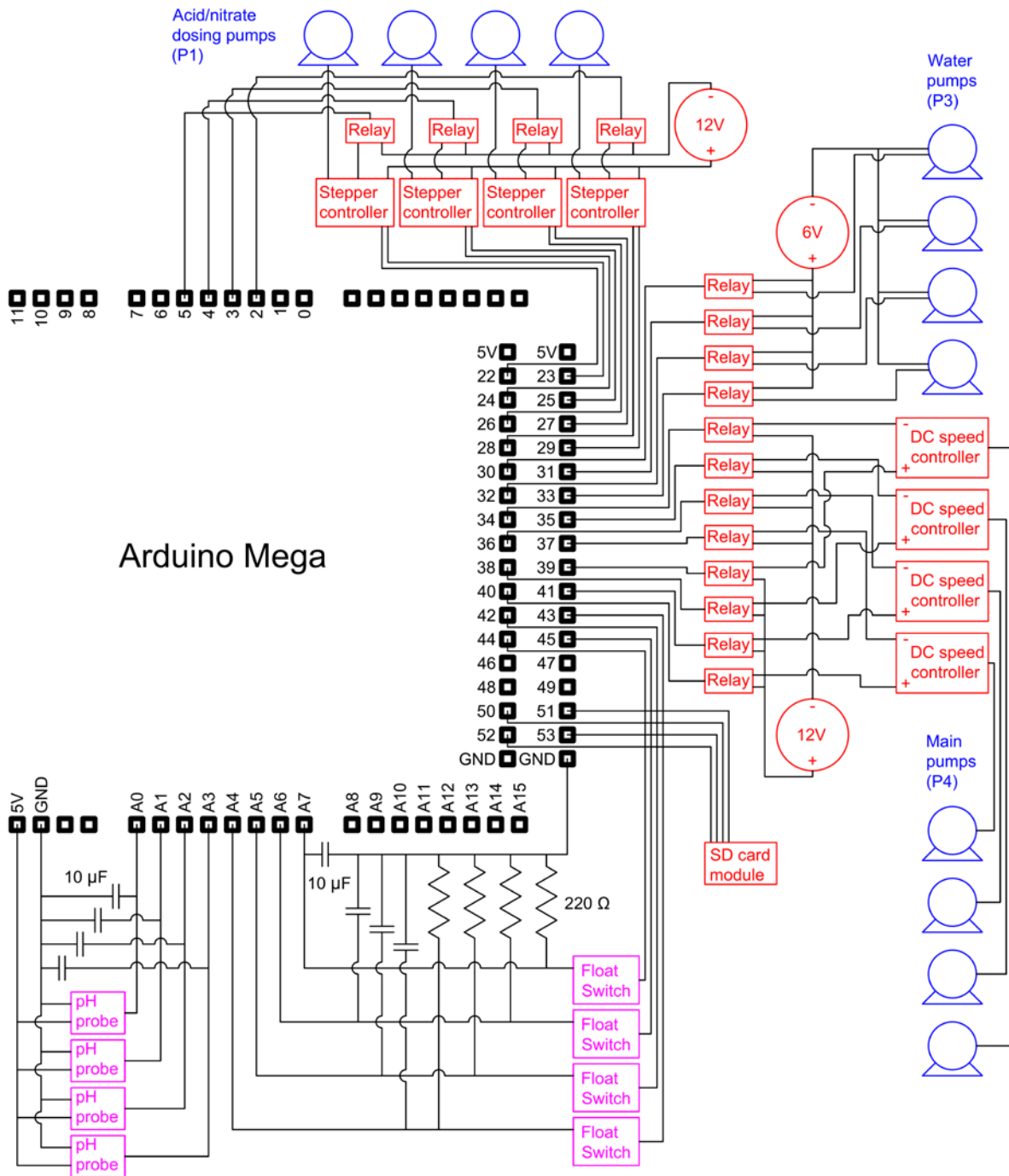


Figure A4. Circuit diagram of the control system.